

Rhodium Containing Magnetic Nanoparticles: Effective Catalysts for Hydrogenation and the 1,4-Addition of Boronic Acids

Urszula Laska · Christopher G. Frost ·
Pawel K. Plucinski · Gareth J. Price

Received: 13 July 2007 / Accepted: 2 November 2007 / Published online: 1 December 2007
© Springer Science+Business Media, LLC 2007

Abstract New efficient rhodium catalysts supported on superparamagnetic iron oxide nanoparticles (NPs) have been prepared using a novel method involving sulfonated triphenylphosphine ligands. They successfully promote the hydrogenation of olefins as well as the addition of aryl-boronic acids to dimethyl itaconate (ItMe₂) in water for up to 10 recycles. The catalysts were stable towards leaching of the metal complexes and were readily recovered by applying an external magnetic field.

Keywords Magnetic nanoparticles · Rhodium catalyst · Catalyst separation

1 Introduction

There has been considerable recent interest in employing dispersed nanoparticles, NPs, as catalysts and supports [1, 2]. Homogeneous catalysts are highly efficient but their separation and recovery from the products can be problematic. Conversely, heterogeneous systems can suffer from lower catalytic activities, generally due to limited mass transport of reactants to the solid surface of the

catalyst [3]. Approaches designed to overcome these drawbacks include using biphasic systems [1] and supporting the active species on membranes [3], polymers [4] or dendrimers [5]. Nanoparticulate supports form a “semi-homogeneous” system and can serve as an intermediate between these types.

One of the most promising nanoparticulate supports for the development of high-performance catalyst supports is superparamagnetic iron oxide. The NPs are attracted to a magnetic field and so may be recovered, but they retain no residual magnetism when the field is removed [6]. Using these NPs offers advantages in “clean” chemistry since, in addition to being readily recovered; they are non-toxic and widely accessible. The NP surface can be functionalized to allow the attachment of catalytically active groups. For example, rhodium species on magnetic NPs (as [Rh(cod)(η^6 -benzoic acid)]BF₄) have been used in the hydroformylation of olefins by Lee et al. [7]. The groups of Gao et al. [8–10] and He [11, 12] recently reported the use of iron oxide–Pd systems as efficient catalysts for certain cross-coupling reactions. Magnetic NPs have also been used as a support for chiral ruthenium complexes that have been applied to the catalytic, asymmetric hydrogenation of aromatic ketones [13].

In this paper, we report a novel method for the preparation of magnetically separable rhodium–phosphine complexes by anchoring to Fe₃O₄ NPs as well as a preliminary assessment of their application as recyclable catalysts for the hydrogenation of alkenes and the 1,4-addition of boronic acids. As far as we are aware, this is the first report of Rh-functionalised magnetic NP catalyst that can be used in water and recycled. An attractive feature of this method is the simplicity of immobilisation procedure since no modification of either the NP support or the organometallic species is required.

U. Laska (✉) · P. K. Plucinski
Department of Chemical Engineering, University of Bath,
Claverton Down, Bath BA2 7AY, UK
e-mail: U.Laska@bath.ac.uk

U. Laska · C. G. Frost · G. J. Price
Department of Chemistry, University of Bath, Claverton Down,
Bath BA2 7AY, UK

2 Experimental Section

2.1 Materials and Instrumentation

[Rh(cod)Cl]₂ (98%), dimethyl itaconate (99%), *trans*-2-phenylvinylboronic acid (97%), 4-biphenylboronic acid, ammonium hydroxide (28% NH₃ in water), hydrochloric acid (37%), and tetrahydrofuran (99.5+%) were purchased from Aldrich. Iron (II) chloride tetrahydrate (99%), iron (III) chloride hexahydrate (99+%), tetramethylammonium hydroxide pentahydrate (99%), phenylboronic acid (98+%), 4-bromophenylboronic acid (98%), 4-methoxyphenylboronic acid (97%), 3,5-dichlorophenylboronic acid, 3-nitrophenylboronic acid (97%) were purchased from Acros Organics, and methanol (HPLC grade), ethyl acetate (LRG), and hexane (LRG) from Fisher Scientific. Sodium 3-(diphenylphosphino)benzenesulfonate (TPPMS) was synthesized applying Ahrlund's modified method [14]. Triphenylphosphine-3,3',3''-trisulfonic acid trisodium salt (precursor of rhodium(I) tris(trisodium triphenylphosphine-3,3',3''-trisulfonate) chloride, [Rh(TPPTS)₃Cl]) was purchased by Fluka. THF and methanol were purified and dried using standard procedures [15]. All remaining reagents and chemicals were used as received.

The size and morphology of resulting nanoparticles were characterized by transmission electron microscopy. Low-magnification TEM images were recorded on JEOL JEM-1200EX II Transmission Electron Microscope (JEOL, Tokyo, Japan) equipped with Gratan Digital Camera & "Digital Micrograph 3.4" Software (Grattan, Oxon, UK). High-resolution HRTEM images were obtained using a JEOL JEM 2010 with LaB₆-Cathode and CCD-Camera (TVIPS). EDX patterns were recorded on a JEOL JSM 5900 LV with wolfram cathode. X-ray diffraction data were obtained using a Philips 4 kW X-ray generator (PW1730) with a CuK α X-ray source ($\lambda = 1.54060$ Å) and the diffractometer goniometer (PW1820) controlled via Philips (PW1877 PC-APD) software. The rhodium contents in supernatants were determined by atomic absorption spectrophotometry (AAS) with a Varian AA 275 atomic absorption spectrophotometer.

2.2 Catalyst Preparation

2.2.1 Synthesis of Iron Oxide Nanoparticles (NPs)

Iron oxide nanoparticles were prepared by a slight modification of the known co-precipitation method [16], in which co-precipitation of ferric and ferrous salts in basic medium is followed by stabilization using OH[−] ions. In a typical synthesis FeCl₃ · 6H₂O (5.4 g, 20 mmol) and FeCl₂ · 4H₂O (2.0 g, 10 mmol) were dissolved under N₂ in

an acidic solution (10.3 mmol HCl in 25 cm³ H₂O), such that Fe³⁺ to Fe²⁺ molar ratio was 2. The as-prepared solution was added dropwise to 250 cm³ of a deoxygenated 1.5 M NH₄OH with vigorous stirring. The black precipitate was isolated from the solvent via magnetic decantation. The washing–decantation procedure was repeated three times followed by washing twice with 100 cm³ of 0.1 M TMAOH. Finally, the suspension was precipitated with acetone and methanol, and the precipitate dried in a desiccator overnight.

2.2.2 Synthesis of [Rh(TPPMS)(cod)Cl]

[Rh(cod)Cl]₂ (25 mg, 0.05 mmol) and TPPMS (36 mg, 0.10 mmol) were dissolved under N₂ in 10 cm³ of dried THF and stirred at room temperature for 1.5 h. The solvent was removed by evaporation to give a yellow solid, which was further dried in vacuum overnight. The solid was used for immobilization without further purification.

2.2.3 Immobilization of Rh Complex onto NPs

[Rh(TPPMS)(cod)Cl] or [Rh(TPPTS)₃Cl] (129 mg, 0.07 mmol) and dry NPs (2.0 g) were placed into a flask and purged with N₂ for 15 min. About 20 cm³ of dried MeOH was added via syringe and the mixture was subjected to ultrasonication using a 30 kHz, 50 W cleaning bath for 3 h. The solid catalyst was separated using an external permanent magnet and washed several times with dried methanol until no Rh in supernatant was detected by means of AAS. The surface coverage of rhodium catalyst on iron oxide nanoparticles was calculated on a basis of AAS measurements of Rh remaining in supernatants and was estimated to be ~48–50 μmol/g (~0.25 mol/nm²).

2.3 General Procedures for Catalytic Reactions

2.3.1 Coupling Reactions

All boronic acid addition reactions were done according to the procedure described in Frost et al. [17, 18]. In a typical reaction, 1 equiv. (32 mg, 0.20 mmol) of dimethyl itaconate, 2 equiv. (0.40 mmol) of arylboronic acid, and 0.30 g of NP-[Rh(TPPMS)(cod)Cl] catalyst (~7 mol% of Rh) were added to 5 cm³ of water. The mixture was refluxed under an air atmosphere for 24 h and aliquots of solution were taken at fixed intervals for GC analysis. The mixture was then cooled to room temperature and the catalyst was separated from the reaction medium using an external permanent magnet and used in the next cycle without

purification. The product was extracted from the aqueous phase using ethyl acetate ($3 \times 5 \text{ cm}^3$). The combined organic phases were washed with brine (15 cm^3) and dried over MgSO_4 . After filtration the solvent was evaporated under vacuum and the product analysed using ^1H NMR.

2.3.2 Hydrogenation

The hydrogenation of dimethyl itaconate (ItMe_2) was carried out in a 50 cm^3 high-pressure stainless steel reactor. The reactor was charged with ItMe_2 (63 mg, 0.40 mmol), $\text{NP-}[\text{Rh}(\text{TPPTS})_3\text{Cl}]$ catalyst (0.35 g), and 20 cm^3 of MeOH and then sealed. It was alternatively purged with N_2 and H_2 four times and finally filled with H_2 up to the pressure of 3.5 bar. The reaction mixture was stirred at 50°C for 4 h. After the reaction time, the reactor was cooled to room temperature and depressurized to atmospheric pressure. The catalyst was separated by magnetic decantation, washed three times with MeOH and used for the subsequent reaction without further purification. The reaction mixture and supernatants after catalyst washing were collected and solvent evaporated under vacuum. Samples were analyzed using ^1H NMR and gas chromatography.

3 Results and Discussion

Scheme 1 shows the route used to prepare the catalyst NPs. Chemical co-precipitation of Fe^{2+} and Fe^{3+} in basic solution yielded magnetite NPs [16]. Rhodium was anchored to the surface by using a complex containing sulfonated ligands, these previously having been shown to have high affinity for the NP surface [19]. Two approaches were used. Firstly, rhodium (I) tris(trisodium triphenylphosphine-3,3',3''-trisulfonate) chloride (synthesized using the method developed by Herrmann et al. [20, 21]; the structure confirmed by comparison of the NMR data¹), $[\text{Rh}(\text{TPPTS})_3\text{Cl}]$ (**1**), was used directly for immobilisation without the necessity of any ligand modification. Secondly, a rhodium precursor, $[\text{Rh}(\text{cod})\text{Cl}]_2$ (cod = 1,5-cyclooctadiene), was reacted with sodium 3-(diphenylphosphino)benzenesulfonate to give $[\text{Rh}(\text{TPPMS})(\text{cod})\text{Cl}]$ (**2**), which could also be easily attached to NPs. AAS analysis of the residual Rh in the supernatant after immobilization showed the Rh loading on the NPs to be $49 \pm 1 \mu\text{mol/g}$, typical of loadings reported by other authors [7–13].

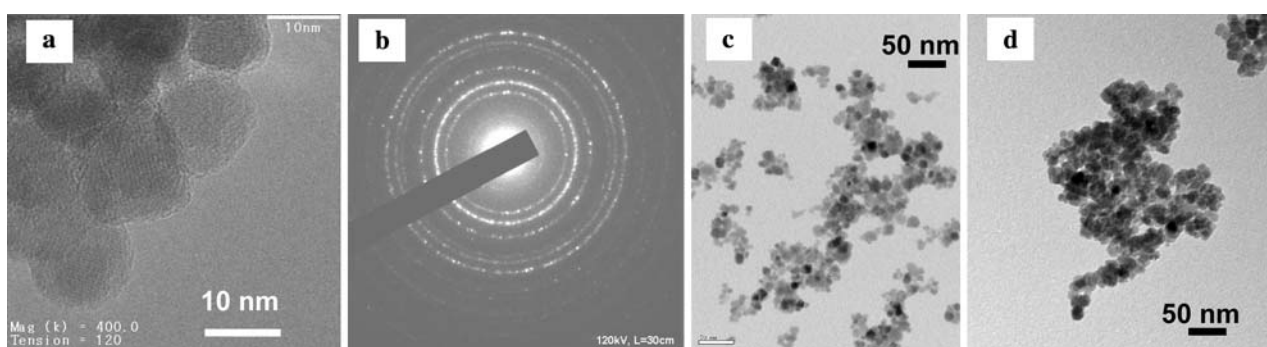
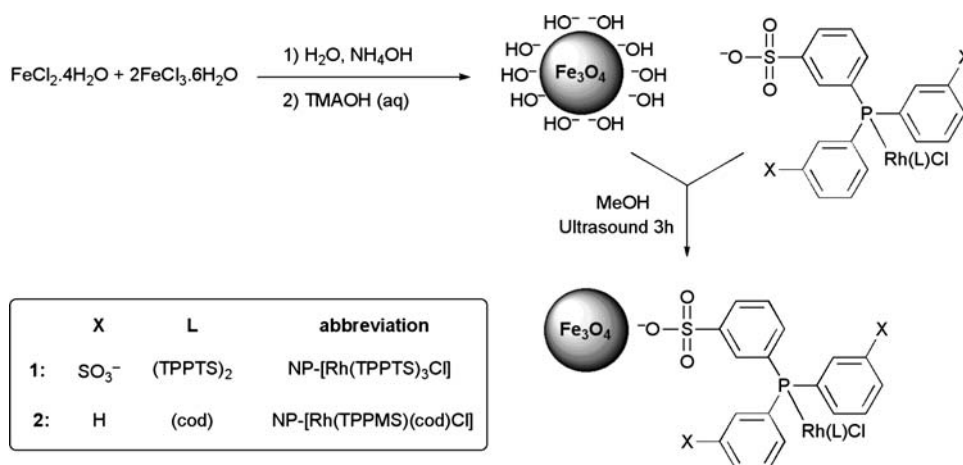
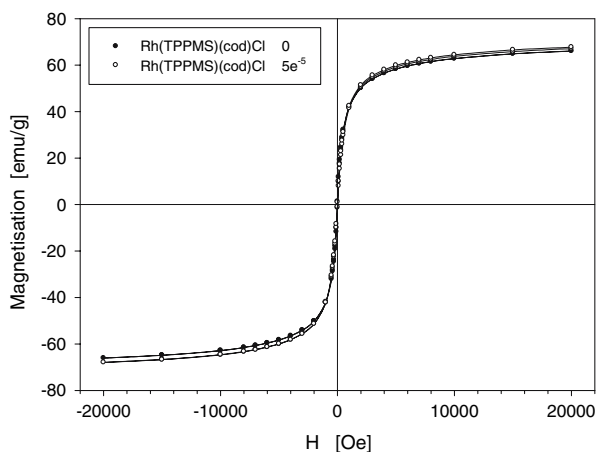
High-resolution TEM micrographs confirmed the formation of a crystalline core coated by an amorphous organic shell, shown by Fig. 1a for $\text{NP-}[\text{Rh}(\text{TPPMS})(\text{cod})\text{Cl}]$. The average particle size was ca. 10 nm, although there was a relatively wide size distribution. Moreover, the pictures show that most of the particles deviate from sphericity, due to the spinel nature of magnetite. Powder X-ray diffraction (XRD) patterns corresponded well to standard magnetite reflections [22] and particle sizes estimated from the Debye–Scherrer formula are consistent with those observed by TEM. The particle composition was confirmed by selected area diffraction (SAD) (Fig. 1b) and energy-dispersive X-ray (EDX) spectra.

Superconducting quantum interference device (SQUID) analysis allowed the characterization of the particle magnetization as well as giving another independent measurement of the iron oxide core size. Figure 2 shows the magnetization curves for the bare NPs and then after functionalisation with $[\text{Rh}(\text{TPPMS})(\text{cod})\text{Cl}]$. The curves were fitted to Langevin equation giving mean particle diameters of $8.7 \pm 4.0 \text{ nm}$ and $8.2 \pm 3.1 \text{ nm}$ for bare and functionalized NPs respectively, agreeing reasonably well with TEM and XRD. As expected for iron oxide NPs, the typical characteristics of superparamagnetic behaviour, zero coercivity and no remanence on hysteresis were observed. Additionally, it can be seen that neither the presence of the organometallic layer nor the immobilisation procedure have any significant effect on the magnetic properties of the NPs.

To investigate the catalytic performance of our catalysts, their activity in single-phase (1,4-addition of boronic acids) and two-phase (hydrogenation) reactions was studied in water with dimethyl itaconate, ItMe_2 , as the substrate (Tables 1, 2). Initial hydrogenation of ItMe_2 using $\text{NP-}[\text{Rh}(\text{TPPTS})_3\text{Cl}]$ at atmospheric pressure and ambient temperature gave 60% conversion (Table 1, entry 1). However, complete conversion was achieved in 4 h by operating at $p(\text{H}_2) = 3.5 \text{ bar}$ and $T = 50^\circ\text{C}$. The catalyst was also tested with *n*-hexene, and *n*-dodecene (Table 1, entries 2 and 3) and showed very good activity with >99% of alkane produced within 4 h and high selectivity. Importantly, no 2-alkene side product from isomerisation was observed. After each reaction, separation of the catalyst was achieved by using an external permanent magnet, from which the reaction mixture was decanted.

Building on the excellent results obtained for hydrogenation, attention was focused on the rhodium catalysed 1,4-addition reaction of boronic acids. Table 2 illustrates the results obtained for the $\text{NP-}[\text{Rh}(\text{TPPMS})(\text{cod})\text{Cl}]$ catalysed conjugate addition of boronic acids to ItMe_2 using the method described by Frost et al. [17, 18]. In each case, excellent conversions were achieved after 24 h irrespective of the electronic nature of the arylboronic acid. Workup was

¹ ^1H NMR (d_6 -acetone, ppm): δ 7.81 (dd, 2H, phenyl sulfonate), 7.46–7.40 (m, 12H, phenyl), 4.10 (s, 4H, cod), 2.47 (m, 4H, cod), 1.81 (m, 4H, cod).

Scheme 1 Preparation of magnetic nanoparticle-supported rhodium catalysts**Fig. 1** TEM micrographs and selected area diffraction (SAD) patterns of iron oxide-supported catalyst NP-[Rh(TPPMS)(cod)Cl]: (a) HRTEM image; (b) SAD pattern; (c) before reaction; (d) after reaction, showing aggregation**Fig. 2** SQUID hysteresis of [Rh(TPPMS)(cod)Cl] functionalised iron oxide NPs (numbers in legend correspond to the catalyst loading—see Fig. 3)

again facilitated since the aqueous phase was simply decanted from the catalyst held in place by an external magnet.

To confirm the role of Rh in the catalysis of both hydrogenation and 1,4-addition reactions, control

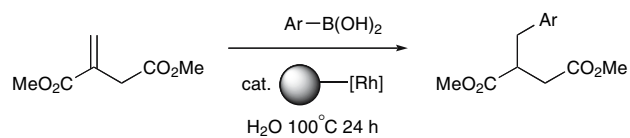
Table 1 Hydrogenation of olefins catalysed by NP-[Rh(TPPTS)₃Cl]

Entry	Substrate	Product	Conversion (%)	
1			60 ^a	100 ^b
2			45 ^a	>99 ^b
3			40 ^a	100 ^b

^a 4 h at $p(\text{H}_2) = 1 \text{ bar}$, $T = 25^\circ\text{C}$

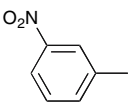
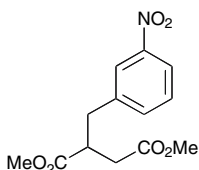
^b $p(\text{H}_2) = 3.5 \text{ bar}$, $T = 50^\circ\text{C}$. All conversions determined by ^1H NMR spectroscopy and gas chromatography

experiments were performed using unfunctionalised NPs. As expected, neither bare iron oxide NPs nor NPs coated only with the phenylphosphine ligands, were active in either reaction under the conditions used herein. Moreover, it is notable that NP-[Rh(TPPMS)(cod)Cl] gave conversions similar to those from the same level of

Table 2 Addition^a of arylboronic acids to dimethyl itaconate catalysed by NP-[Rh(THPPMS)(cod)Cl]

Entry	Ar	Product	Conversion (%)	
			4 h	24 h
1			100	100
2			84	>99
3			80	99
4			91	99
5			9	97
6			30	96

Table 2 continued

Entry	Ar	Product	Conversion (%)	
			4 h	24 h
7			40	92

^a Reaction conditions: NPs loaded with [Rh(PPMS)(cod)Cl] were added (7 mol% Rh) to dimethyl itaconate (1.0 equiv.) and boronic acid (2.0 equiv.) in water. The mixture was stirred at 100 °C and the catalyst separated using an external magnet. The product was extracted with EtOAc

^b Determined by ¹H NMR spectroscopy and gas chromatography

homogeneous [Rh(PPMS)(cod)Cl] (96% conversion after 4 h) and also comparable with those of the parent rhodium precursor [Rh(cod)Cl]₂ (100%) under the same reaction conditions.

The influence of catalyst loading on the magnetic NPs was also investigated for NP-[Rh(PPMS)(cod)Cl] catalysed 1,4-addition of phenylboronic acid to ItMe₂ (Fig. 3). Under the dry conditions of TEM analysis, the increase of catalytic layer around the nanoparticles is clearly evident. Analysis of results shown in Fig. 4 suggests the existence of an optimum coverage, above which the reactivity of the catalyst is almost constant. Further increase of catalytic loading does not influence the catalyst performance; however it can influence the economy of the process in terms of the cost of a catalyst. The detailed analysis of the kinetics over the first hour was studied for three catalyst scenarios shown schematically on Fig. 5. The measured kinetic results were interpreted assuming: (i) second order reaction (Eq. 1a), and (ii) the linear influence of the catalyst concentration on the reaction rate (Eq. 1b).

$$\begin{aligned} \text{a: } (-r_A) &= k_{\text{app}} \cdot c_A c_B \\ \text{b: } k_{\text{app}} &= k^* \cdot c_{\text{cat}} \end{aligned} \quad (1)$$

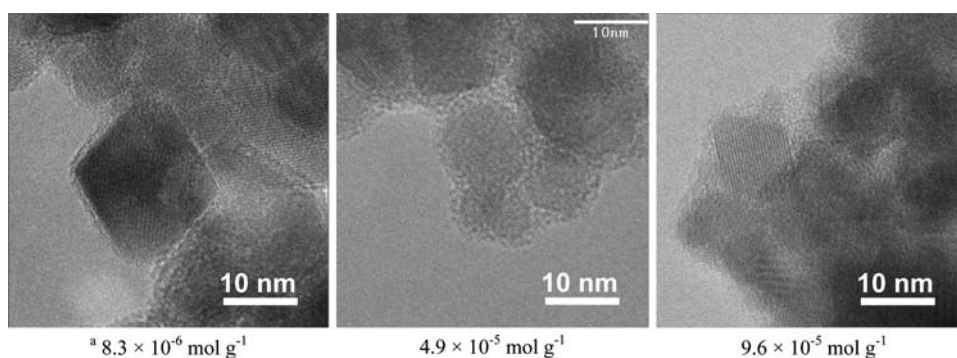
where $(-r_A)$ = rate of reactant (phenylboronic acid) disappearance, k_{app} = apparent second order kinetic constant, c_{cat} = catalyst concentration, k^* = kinetic constant, c = concentration.

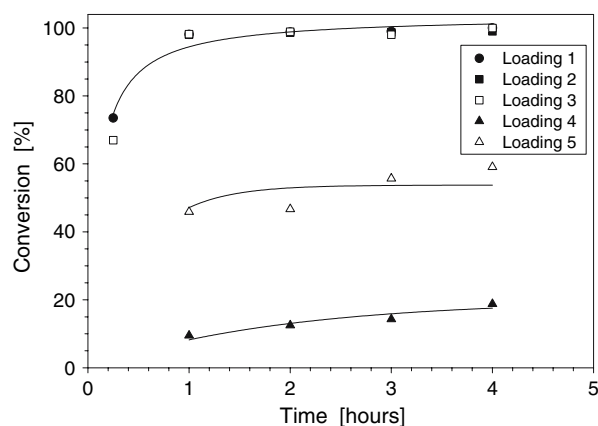
The increase of the mass of catalyst (from 3.6 to 7.0 mol%), keeping the same catalyst loading (as moles of [Rh(PPMS)(cod)Cl] per gram of nanoparticles) resulted with almost the same rate constant (compare catalysts 1 and 2), which is in agreement with principles of homogeneous catalysis (concentration independent kinetic constant). However, the immobilisation of thicker layer of catalyst resulted in a higher rate constant (catalyst 3, Fig. 5). It could be that a thicker organic layer stabilises the nanoparticles in the reaction medium, so less agglomeration took place and the resulting reactivity was higher.

The facile magnetic separation and recovery of the NPs gives great potential for the recycling and repeated use of the catalyst. We have successfully reused NP-[Rh(TPPTS)₃

Fig. 3 HRTEM images of magnetic nanoparticles with various loading of [Rh(PPMS)(cod)Cl].

^a Moles of Rh per mass of iron oxide nanoparticles





Loading	Rh ^a mol/g NP	Rh ^b mol/g NP	Rh ^c mol %
1) ●	1·10 ⁻⁴	9.6·10 ⁻⁵	7.0
2) ■	5·10 ⁻⁵	4.9·10 ⁻⁵	3.6
3) □			7.0
4) ▲	1·10 ⁻⁵	8.3·10 ⁻⁶	3.6
5) △			7.0

Fig. 4 The influence of catalyst loading (amount of Rh per mass of NPs) on the conversion of dimethyl itaconate. ^a Initial Rh amount, ^b immobilised Rh amount, ^c mol% of Rh in the system

Cl] for 10 cycles of ItMe₂ hydrogenation without any loss of activity (see Table 3). The catalyst efficiency was maintained even when repeatedly employed over the course of several days with no special treatment. NPs were used in air and washed three times with MeOH to remove the product. In case of phenylboronic acid addition, further aliquots of reactant added at 4 h intervals showed that

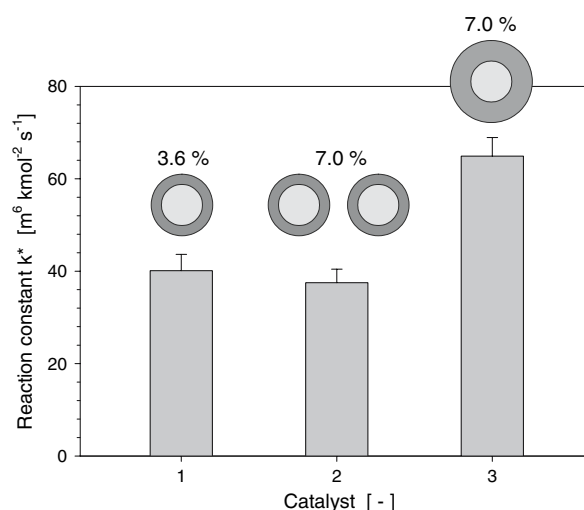


Fig. 5 The influence of catalyst loading on the reaction kinetic constant (the same condition as in Fig. 4). Note: Catalyst 1 corresponds to loading 2 in Fig. 4, catalyst 2 corresponds to loading 3, and catalyst 3 corresponds to loading 1

NP-[Rh(THPPMS)(cod)Cl] retained activity, giving conversions of 93% for the second addition and 53% for the fifth. These results suggest that the catalyst may be suitable for a continuous flow reaction system. Recovery of the catalyst after the first 4 h reaction and subsequent reuse was a less successful approach. After decanting the aqueous phase, the catalyst held by an external magnet was washed, dried under nitrogen and used for a subsequent run of the same reaction without further treatment. More than 96% of the mass of NP-[Rh(THPPMS)(cod)Cl] was recovered. Washing with water led to a low conversion (15%) in the second run. GC analyses of the supernatant after each washing showed no product remained in solution. TEM observation of these catalyst NPs after a repeat run showed evidence of some particle agglomeration (compare Fig. 1c,

Table 3 Magnetic supported catalysts recycling

Catalyst	Reaction	Conversion
NP-[Rh(THPPMS) ₃ Cl]		100% 10 consecutive runs of catalyst
NP-[Rh(THPPMS)(cod)Cl]		Washing 1st run: >99% 2nd run: 63.8% Continuous 1st run: >99% 2nd run: 92.7%

d) which could explain the reduction of catalytic activity. In both cases (ligands **1** and **2**), AAS analysis for Rh (detection limit 0.1 ppm) in reaction mixture suggested that no catalyst leaching occurred, a conclusion supported by the lack of ligand signals seen in the NMR spectra of products.

4 Conclusions

In summary, we have demonstrated a simple procedure for the preparation of novel magnetic nanoparticle-supported rhodium catalysts using sulfonated ligands which eliminate the need for intermediate treatments of the nanoparticles prior to functionalisation. The anchored $[\text{Rh}(\text{TPPTS})_3\text{Cl}]$ catalyst can be readily separated in magnetic field and used for olefin hydrogenation more than 10 times without loss of activity. The NP- $[\text{Rh}(\text{TPPMS})(\text{cod})\text{Cl}]$ system also efficiently catalyses the aqueous reaction of dimethyl itaconate and arylboronic acids. While further optimisation is necessary, the systems show good potential as recyclable catalysts for clean synthesis. The simplicity of the presented catalyst immobilisation approach, the remarkably high catalytic activity as well as the easy separation procedure are promising directions for designing of other efficient nanomagnet-based systems for a range of catalytic reactions.

Acknowledgments We gratefully acknowledge financial support from EPSRC (Engineering Functional Materials, EP/C519736/1) and thank the Centre for Electron Optical Studies at Bath for TEM and the Department of Physics at Bath for XRD. We are also grateful to Dr. A. Garcia Prieto at University College, London, for SQUID measurements as well as Prof. S. Weinkauf and Dr. M. Hanzlik at the Technical University of Munich for further assistance with HRTEM.

References

1. Astruc D, Lu F, Aranzas JR (2005) *Angew Chem Int Ed* 44:7852
2. Bedford RB, Betham M, Bruce DW, Davis SA, Frost RM, Hird M (2006) *Chem Commun* 1398
3. Cole-Hamilton DJ (2003) *Science* 299:1702
4. Leadbeater NE, Marco M (2002) *Chem Rev* 102:3217
5. Angurell I, Muller G, Rocamora M, Rossell O, Seco M (2003) *Dalton Trans* 1194
6. Berkovski B (1996) In: Berkovski B, Bashtovoy V (eds) *Magnetic fluids and applications handbook*, ch. 1. Begell House, Inc., New York, pp 1–250
7. Yoon T-J, Lee W, Oh Y-S, Lee J-K (2003) *New J Chem* 27:227
8. Stevens PD, Fan J, Gardimalla HMR, Yen M, Gao Y (2005) *Org Lett* 7:2085
9. Stevens PD, Li G, Fan J, Yen M, Gao Y (2005) *Chem Commun* 4435
10. Zheng Y, Stevens PD, Gao Y (2006) *J Org Chem* 71:537
11. Wang Z, Xiao P, Shen B, He N (2006) *Colloids Surf A* 276:116
12. Wang Z, Shen B, Aihua Z, He N (2005) *Chem Eng J* 113:27
13. Hu A, Yee GT, Lin W (2005) *J Am Chem Soc* 127:12486
14. Suárez T, Fontal B, Reyes M, Bellandi F, Contreras RR, Bahsas A, León G, Cancines P, Castillo B (2004) *React Kinet Catal Lett* 82:317
15. Riddick JA, Bunger WB, Sakano TK (1986) *Organic solvents: physical properties and methods of purification*, 4th edn. Wiley, New York
16. Lyon JL, Fleming DA, Stone MB, Schiffer P, Williams ME (2004) *Nano Lett* 4:719
17. Wadsworth KJ, Wood FK, Chapman CJ, Frost CG (2004) *Synlett* 2022
18. Moss RJ, Wadsworth KJ, Chapman CJ, Frost CG (2004) *Chem Commun* 1984
19. Yee C, Kataby G, Ulman A, Prozorov T, White H, King A, Rafailovich M, Sokolov J, Gedanken A (1999) *Langmuir* 15:7111
20. Herrmann WA, Kulpe JA, Kellner J, Riepl H, Bahrmann H, Konkol W (1990) *Angew Chem* 102:408
21. Herrmann WA, Kulpe JA, Konkol W, Bahrmann H (1990) *J Organomet Chem* 389:85
22. Hyeon T, Lee SS, Park J, Chung Y, Na HB (2001) *J Am Chem Soc* 123:12798